The anticancer effects of cinobufagin on hepatocellular carcinoma Huh-7 cells are associated with activation of the p73 signaling pathway

LEI ZHAO[1,2*], LINA FU[3*], ZHONGWEI XU[1], RONG FAN[1], RUICHENG XU[1], RONG FU[1], SHUANG ZOU[1], CONGCONG WANG[1], YAN ZHANG[1], JIABAO WANG[1], JUN BAO[1], ZHIMEI WANG[1], XIAOJIE HOU[1], YUPIAO ZHENG[4], ERQING DAI[2] and FENGMEI WANG[4]

[1]Central Laboratory, Logistics University of Chinese People's Armed Police Force, Tianjin 300309; [2]Hepatology Department of Pingjin Hospital, Logistics University of Chinese People's Armed Police Forces, Tianjin 300162; [3]Department of Gastroenterology, Tianjin Fourth Central Hospital, Tianjin 300140; [4]Department of Gastroenterology and Hepatology, The Third Central Hospital of Tianjin, Tianjin 300170, P.R. China

Received July 12, 2018; Accepted February 14, 2019

DOI: 10.3892/mmr.2019.10108

Abstract. The Na^+/K^+-ATPase inhibitor cinobufagin exhibits numerous anticancer effects on hepatocellular carcinoma (HCC) cells expressing wild-type p53 via inhibition of aurora kinase A (AURKA) and activation of p53 signaling. However, the effects of cinobufagin on HCC cells expressing mutant p53 remain unclear. In the present study, the anticancer effects of cinobufagin were investigated on HCC Huh-7 cells with mutant p53, and the effects of AURKA overexpression or inhibition on the anticancer effects of cinobufagin were analyzed. Viability, cell cycle progression and apoptosis of cells were determined using an MTT assay, flow cytometry and Hoechst 33342 staining, respectively. The expression levels of p53 and p73 signaling-associated proteins were investigated via western blot analysis. The results demonstrated that the expression levels of AURKA, B-cell lymphoma 2 (Bcl-2), cyclin-dependent kinase 1, cyclin B1, proliferating cell nuclear antigen and heterogeneous nuclear ribonucleoprotein K, as well as the phosphorylation of p53 and mouse double minute 2 homolog, were significantly decreased in Huh-7 cells treated with 5 μmol/l cinobufagin for 24 h. Conversely, the expression levels of Bcl-2-associated X protein, p21, p53 upregulated modulator of apoptosis and phorbol-12-myristate-13-acetate-induced protein 1, were significantly increased by cinobufagin treatment. Overexpression or inhibition of AURKA suppressed or promoted the anticancer effects of cinobufagin on Huh-7 cells, respectively. These results indicated that cinobufagin may induce anticancer effects on Huh-7 cells via the inhibition of AURKA and p53 signaling, and via the activation of p73 signaling, in an AURKA-dependent manner.

Correspondence to: Professor Erqing Dai, Hepatology Department of Pingjin Hospital, Logistics University of Chinese People's Armed Police Forces, 220 Chenglin Road, Dongli, Tianjin 300162, P.R. China
E-mail: 13502136445@163.com

Dr Fengmei Wang, Department of Gastroenterology and Hepatology, The Third Central Hospital of Tianjin, 83 Jintang Road, Tianjin 300170, P.R. China
E-mail: yunaixu@163.com

*Contributed equally

Abbreviations: AURKA, aurora kinase A; CG, cardiac glycoside; HCC, hepatocellular carcinoma; NKA, Na^+/K^+-ATPase; TSG, tumor suppressor gene

Key words: cinobufagin, HCC, Aurka, p53, p73

Introduction

Hepatocellular carcinoma (HCC) is the third most common malignancy and second leading cause of cancer-associated mortality worldwide (1). Notably, only 10-20% of patients with HCC can be treated surgically, whereas the majority of patients are treated exclusively with chemotherapy (2). In addition, the various genetic backgrounds of individuals lead to unsatisfactory outcomes following chemotherapy. Cinobufagin, a natural inhibitor of Na^+/K^+-ATPase (NKA), is a cardiac glycoside (CG) that exhibits potential anticancer activity (3,4). A clinical trial revealed that the interaction between digoxin and cisplatin had a synergistic effect on cervical cancer cells (5).

Numerous studies have reported that mutations in various genes can markedly alter the efficacy of chemotherapy, including p53, B-Raf proto-oncogene, serine/threonine kinase and erb-b2 receptor tyrosine kinase 2 (6-9). Mutations in p53 occur frequently in numerous types of malignant tumor (10-12). HCC cells have been reported to express three genotypes of p53: Wild-type p53, mutant p53 and p53-null (13). Our previous study revealed that CGs induce cell cycle S phase arrest and lead to chromosome segregation distortion in HCC HepG2 cells expressing wild-type p53 by inhibiting the function of aurora kinase A (AURKA) and activating p53 signaling (14).

As a member of the aurora kinase family, AURKA is a serine/threonine kinase, which primarily serves roles in regulation of the cell cycle, separation and maturation of centrosomes, and establishment of the spindle. Numerous studies have reported the abnormal amplification and overexpression of AURKA in various types of malignant tumor, including liver, lung and breast cancer (15-18). The overexpression of AURKA is associated with aggressive, poorly differentiated tumors (19,20). p53 is a tumor suppressor gene (TSG) downstream of AURKA that is involved in the regulation of cellular activities via phosphorylation, including cell cycle arrest, DNA repair and apoptosis (21). Various mutations in p53 have been reported in malignant tumors; >50% of mutations are in the form of single nucleotide mutations (22). Mutant p53 loses its TSG function and acts as an oncogene, promoting the proliferation of tumor cells, increasing the invasive and metastatic abilities of tumor cells, and inducing resistance to chemotherapy (23). Notably, p73, a member of the p53 family, can be activated to perform TSG functions in place of the mutant p53, regulating the transcription of p21, growth arrest and DNA damage-inducible protein 45 and B-cell lymphoma 2 (Bcl-2)-associated X protein (Bax) (24). The effects of cinobufagin on HCC cells expressing mutant p53 and the underlying mechanisms remain unclear. Therefore, the anticancer properties of cinobufagin in Huh-7 cells with mutant p53 were investigated in this study.

Materials and methods

Chemicals and reagents. Cinobufagin (cat. no. C1272-1MG) and the rabbit polyclonal anti-phosphorylated (p)-p53 (S315; cat. no. SAB4504500) antibody were purchased from Sigma-Aldrich (Merck KGaA, Darmstadt, Germany). Dulbecco's modified Eagle's medium (DMEM) and fetal bovine serum (FBS) were purchased from Gibco (Thermo Fisher Scientific, Inc., Waltham, MA, USA). The AURKA inhibitor PF-03814735 and the following antibodies were purchased from Abcam (Cambridge, UK): Rabbit monoclonal anti-p21 (cat. no. ab109520), anti-p73 (cat. no. ab40658), anti-mouse double minute 2 homolog (MDM2; cat. no. ab178938), anti-p-p53 (S392; ab33889), rabbit polyclonal anti-p-heterogeneous nuclear ribonucleoprotein K (hnRNPK; S284; cat. no. ab74066), anti-p53 upregulated modulator of apoptosis (PUMA; cat. no. ab9643), mouse monoclonal anti-β-actin (cat. no. ab8226), anti-phorbol-12-myristate-13-acetate-induced protein 1 (Noxa; cat. no. ab13654) anti-hnRNPK (cat. no. ab39975), rabbit monoclonal anti-Bcl-2 (cat. no. ab32124), rabbit monoclonal anti-Bax (cat. no. ab32503), rabbit monoclonal anti-CDK1 (cat. no. ab18), rabbit monoclonal anti-CylinB1 (cat. no. ab32053) and rabbit monoclonal anti-PCNA (cat. no. ab92552).

The rabbit monoclonal anti-AURKA (cat. no. 14475), rabbit polyclonal anti-p-p73 (Y99; cat. no. 4665) and anti-p-MDM2 (S166; cat. no. 3521) antibodies were purchased from Cell Signaling Technology, Inc. (Danvers, MA, USA). The mouse monoclonal anti-p53 (cat. no. MF267038) antibody was purchased from Mei5 Biotechnology, Co., Ltd. (Beijing, China). The propidium iodide (PI) kit (cat. no. Y-6002-T), dimethyl sulfoxide (DMSO; cat. no. D8370) and MTT reagents (cat. no. M1020) were purchased from Beijing Solarbio Science & Technology Co., Ltd. (Beijing, China). The PrimeSTAR® HS DNA Polymerase (cat. no. R010Q) was purchased from Takara Bio, Inc., Otsu, Japan.

Cell culture. Huh-7 cells (possessing an Tyr220Cys point mutation in the p53 gene) (25,26) were purchased from the American Type Culture Collection (Manassas, VA, USA) and were cultured in DMEM supplemented with 10% FBS, penicillin (100 U/ml) and streptomycin (100 μg/ml). The cells were cultured at 37˚C in a humidified 5% CO_2 atmosphere.

Cell transfection. Full-length AURKA cDNA was obtained from Huh-7 cells via polymerase chain reaction (PCR) using the following primer pairs: Forward 5'-CGGGATCCATGG ACCGATCTAAG-3' and reverse, 5'-CCGCTCGAGCTA AGACTGTTTGCTAG-3'. The PCR was performed in a 50 μl volume with PrimeSTAR® HS DNA Polymerase mix (Takara Bio, Inc.). The PCR was performed in a GeneAMP®PCR System 9700 (Applied Biosystems; Thermo Fisher Scientific, Inc.), according to the following protocol: 5 min at 95˚C and 35 cycles of 10 sec at 98˚C, 15 sec at 60˚C and 2 min at 72˚C, followed by 10 min at 72˚C. The PCR product, flanked by *Bam*HI and *Xho*I sites, was cloned into a pCDNA3.1-3xFlag plasmid (BioVector NTCC Inc., Beijing, China) to construct the expression vector pCDNA3.1x3Flag-AURKA. Huh-7 cells were cultured in 6-well plates overnight and were transfected with 2 μg pCDNA3.1x3Flag-AURKA or blank vector using 5 μl Lipofectamine® 3000 reagent (Invitrogen; Thermo Fisher Scientific, Inc.) at 37˚C for 36 h. Stable Huh-7/AURA cell lines were established using 1,000 μg/ml G418 for screening. Huh-7 cells treated with the Huh-7 cells treated with the 50 nmol/l AURKA inhibitor PF-03814735 at 37˚C for 24 h were termed the Huh7/PF-03814735 group. A series of experiments included six groups, including Huh-7, Huh-7/AURKA and Huh-7/PF-03814735 cells, untreated or co-treated with 5 μmol/l cinobufagin at 37˚C for 24 h.

Cell viability assay. An MTT assay was performed to determine cell viability. A total of $5x10^3$ cells suspended in 100 μl DMEM supplemented with 10% FBS were seeded into 96-well plates and cultured for 24 h. The medium was replaced with fresh DMEM containing 10% FBS and various concentrations of cinobufagin (0.75, 1.25, 2.5, 5 and 10 μmol/l). After treatment with cinobufagin or both 5 μmol/l cinobufagin and 50 nmol/l PF-03814735 at 37˚C for 24 h, MTT reagent (20 μl) was added to each well, and the plate was incubated for a further 3 h. Subsequently, the medium was discarded, 100 μl DMSO was added, and the optical density (OD) at 490 nm was detected using an immunosorbent assay microplate reader (SpectraMax M2; Molecular Devices, LLC, Sunnyvale, CA, USA). Cell viability rates were calculated using the following equation: Inhibitory rate (IR) (%)=100x $[(OD_{Treatment}-OD_{Blank})/(OD_{Control}-OD_{Blank})]$. The half maximal inhibitory concentration (IC_{50}) of cinobufagin in Huh-7 cells was also calculated. Another MTT assay was subsequently performed using transfected or 50 nmol/l PF-03814735-treated cells in the presence or absence of 5 μmol/l cinobufagin, according to the aforementioned method.

Cell apoptosis assay. Cells were seeded into 6-well plates at a density of $5x10^4$ cells/well and were cultured for 12 h followed

by treatment with 5 μmol/l cinobufagin and/or 50 nmol/l PF-03814735 at 37˚C for 24 h. Cells were washed with ice-cold PBS and were subsequently incubated with 10 μg/ml Hoechst 33342 at 37˚C for 10 min. Chromatin condensation was observed under a fluorescence microscope (BX41; Olympus Corporation, Tokyo, Japan).

Cell cycle analysis. Cells were trypsinized and fixed in a mixture of 75% ethanol and 25% PBS at 4˚C for 10 min. A total of $2x10^5$ cells were incubated for 45 min with a solution containing 25 μg/ml PI and 40 μg/ml RNase A at 37˚C. The cell cycle distribution was detected using a flow cytometer (FACSCalibur; BD Biosciences, Franklin Lakes, NJ, USA) and analyzed using FlowJo V10 software (FlowJo LLC, Ashland, OR, USA).

Western blot analysis. Cells were cultured until they reached 85% confluence and were then treated with 5 μmol/l cinobufagin at 37˚C for 12 h in the presence or absence of 50 nmol/l PF-03814735. Subsequently, cells were lysed in radioimmunoprecipitation assay buffer [50 mmol/l Tris-HCl (pH 7.4), 150 mmol/l NaCl, 1 mmol/l EDTA, 5% (v/v) β-mercaptoethanol, 1% (v/v) NP-40, 0.25% (v/v) sodium deoxycholate, complete protease inhibitor cocktail (cat. no. P8340; Sigma-Aldrich; Merck KGaA], ultrasonicated at 25% maximum power (20 kHz) (10 sec burst and 20 sec rest, 30 cycles) for 15 min on ice and centrifuged at 4˚C with 13,000 x g for 10 min. The supernatant was collected and stored at -80˚C. Total protein concentration was determined using the bicinchoninic acid assay (Pierce; Thermo Fisher Scientific, Inc.). Protein lysates (60 μg/lane) were separated by 10% SDS-PAGE and transferred to nitrocellulose membranes. The membranes were blocked using 5% bovine serum albumin (BSA; cat. no. 0218054950; GE Healthcare Life Sciences, Little Chalfont, UK) for 1 h at 37˚C and incubated with the primary antibodies at a dilution of 1:1,000 overnight at 4˚C. After four washes with PBS/0.1% Tween 20, the membranes were incubated at room temperature for 1 h with horseradish peroxidase-conjugated secondary antibodies (1:5,000; cat. no. 01-15-06; KPL, Inc., Gaithersburg, MD, USA). Protein bands were visualized using an enhanced chemiluminescence immunoblotting reagent (EMD Millipore, Billerica, MA, USA), and signals were captured using the Amersham Imager 600 system (GE Healthcare Life Sciences, Little Chalfont, UK). Protein expression was semi-quantified using Scion Image version 4.0 (Scion Corporation, Frederick, MD, USA), with β-actin as the reference control.

Immunofluorescence and confocal microscopy. A total of $3x10^3$ cells were seeded onto confocal dishes and treated as aforementioned. Cells were fixed in 4% paraformaldehyde in PBS at 4˚C for 30 min and then permeabilized with 0.5% Triton X-100 in PBS. Cells were blocked with 5% BSA in PBS at room temperature for 1 h and were then incubated with rabbit anti-p73 (1:1,000) overnight at 4˚C, followed by incubation with a fluorescein isothiocyanate-conjugated goat anti-rabbit immunoglobulin G antibody (1:200; cat. no. 5230-0301; KPL, Inc.) at 37˚C for 1 h. Cells were washed three times with PBS (10 min/wash), and the fluorescence was visualized using laser scanning confocal microscopy (Leica TCS SP8; Leica Microsystems GmbH, Wetzlar, Germany). The gray intensity of the images was analyzed using Image-Pro Plus 6.0 software (Media Cybernetics, Inc., Rockville, MD, USA).

Statistical analysis. Data were analyzed using SPSS version 22.0 software (IBM Corp., Armonk, NY, USA). Data were analyzed using one-way analyses of variance followed by a Tukey's test against the control group to adjust for multiple comparisons. Data were presented as the means ± standard error of the mean of three independent experiments. $P<0.05$ was considered to indicate a statistically significant difference.

Results

Decreased viability of Huh-7 cells following cinobufagin treatment is associated with AURKA activity. An MTT assay was performed to analyze the effects of cinobufagin on the viability of Huh-7 cells. As presented in Fig. 1A, treatment with >0.75 μmol/l cinobufagin significantly decreased the viability of cells compared with the control ($P<0.05$). The viability rate of the control group was normalized as 100%, and the viability rates of Huh-7 cells following treatment with 0.75, 1.25, 2.5, 5 and 10 μmol/l cinobufagin for 24 h were reduced by 24.1±3.2, 28.1±3.5, 39.1±3.8, 49.3±4.1 and 60.3±5.22%, respectively. The IC_{50} value of cinobufagin in Huh-7 cells was determined to be 5.1 μmol/l at 24 h. Following treatment with 5 μmol/l cinobufagin for 24 h, the viability rate of Huh-7 cells was determined to be 49.5±3.9% compared with that of the control group; however, transfection with the AURKA expression vector significantly increased the viability rate of Huh-7 cells to 73.6±2.2% (Fig. 1B). Conversely, treatment with 50 nmol/l PF-03814735 significantly decreased the cell viability rate to 41.9±2.2%. The results of the MTT assay indicated that cinobufagin inhibited the viability of mutant p53 HCC cells. Additionally, overexpressing and inhibiting AURKA inhibited and promoted the anti-viability effects of cinobufagin on Huh-7 cells, respectively.

Cinobufagin-induced apoptosis of Huh-7 cells is associated with AURKA activity. Hoechst 33342 staining revealed that the nuclear morphologies of Huh-7 and Huh-7/AURKA cells presented uniform blue fluorescence, dispersed chromatin and oval nuclei, whereas cells treated with cinobufagin and/or PF-03814735 detached from the culture plate, shrunk and formed small apoptotic bodies (Fig. 2A). Other characteristics of apoptosis were also observed following cinobufagin treatment, including nuclear condensation and fragmentation. The proportion of apoptotic cells in the PF-03814735, cinobufagin and PF-03814735 + cinobufagin groups were significantly increased compared with in the control group ($P<0.05$); however, there was no significant difference between the control and Huh-7/AURKA groups. Furthermore, the proportion of apoptotic cells in the PF-03814735 + cinobufagin group was significantly increased compared with in the cinobufagin group ($P<0.05$), whereas that in the Huh-7/AURKA + cinobufagin group was significantly decreased ($P<0.05$). Western blot analysis revealed that cinobufagin treatment significantly downregulated the expression levels of the antiapoptotic protein Bcl-2 in Huh-7 cells compared with the control, and upregulated those of the proapoptotic protein Bax ($P<0.05$; Fig. 2B). In addition,

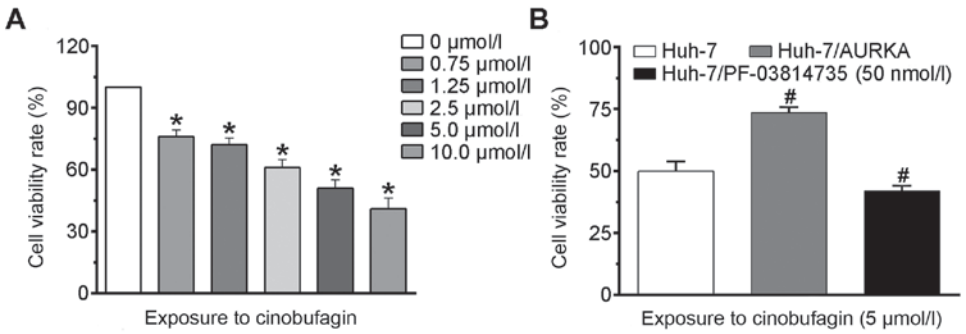

Figure 1. Cinobufagin inhibits the viability of Huh-7 cells in an AURKA-dependent manner. (A) Effects of treatment with various doses of cinobufagin for 24 h on the viability of Huh-7 cells, as determined using an MTT assay. The half maximal inhibitory concentration of cinobufagin in Huh-7 cells was determined to be 5.1 μmol/l. (B) Effects of overexpression or PF-03814735-mediated (50 nmol/l) inhibition of AURKA on the anti-viability effects of 5 μmol/l cinobufagin on Huh7 cells. Data are presented as the means ± standard error of the mean of three independent experiments. *P<0.05 vs. 0 μmol/l; #P<0.05 vs. Huh-7. AURKA, aurora kinase A.

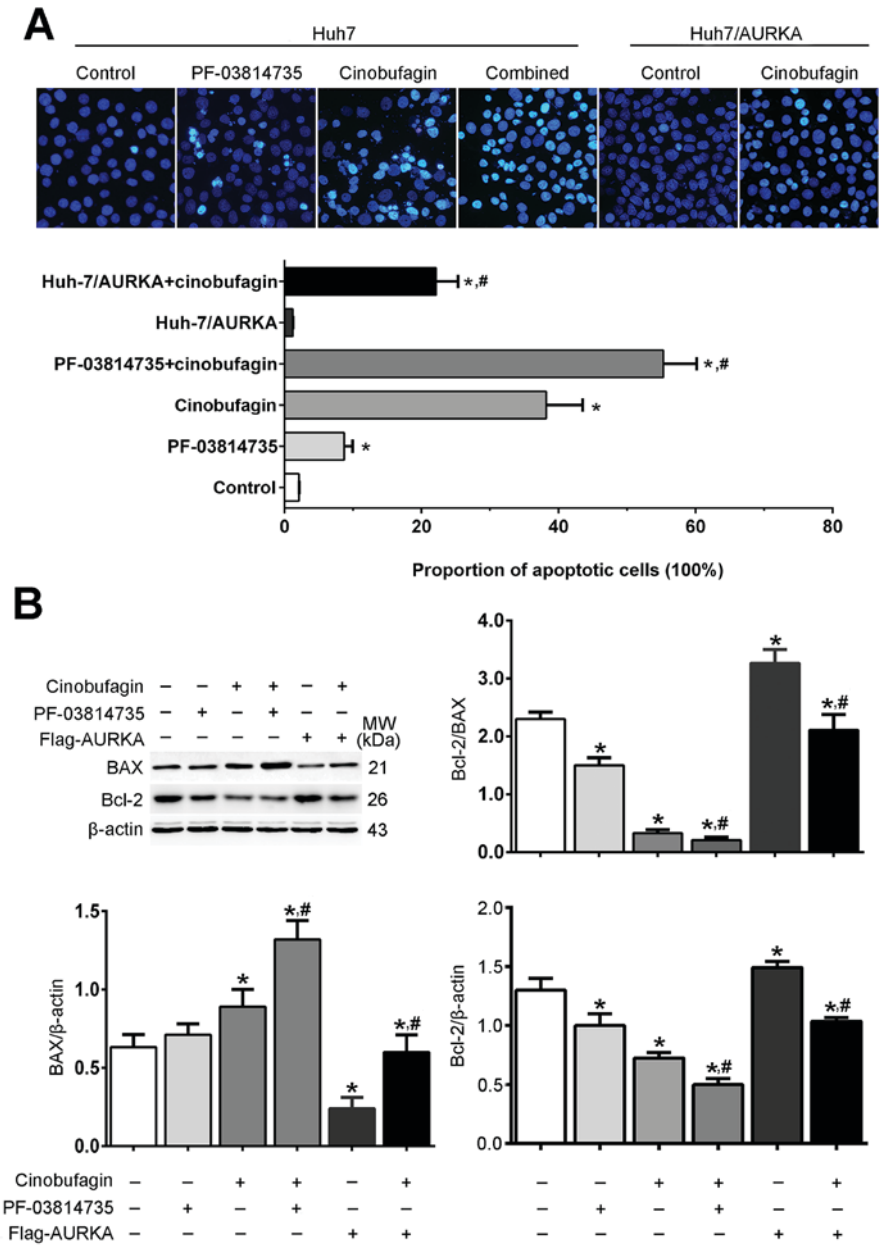

Figure 2. Cinobufagin induces apoptosis of Huh-7 cells. (A) Representative images of Hoechst 33342 staining (magnification, x200). Cells treated with cinobufagin presented various characteristics of apoptosis, including nuclear condensation and fragmentation. (B) Protein expression levels of Bax and Bcl-2, and the ratio of Bax/Bcl-2, as determined by western blotting. β-actin was used as a control. Data are presented as the means ± standard error of the mean of three independent experiments. *P<0.05 vs. control, #P<0.05 vs. cinobufagin. AURKA, aurora kinase A; Bax, Bcl-2-associated X protein; Bcl-2, B-cell lymphoma 2.

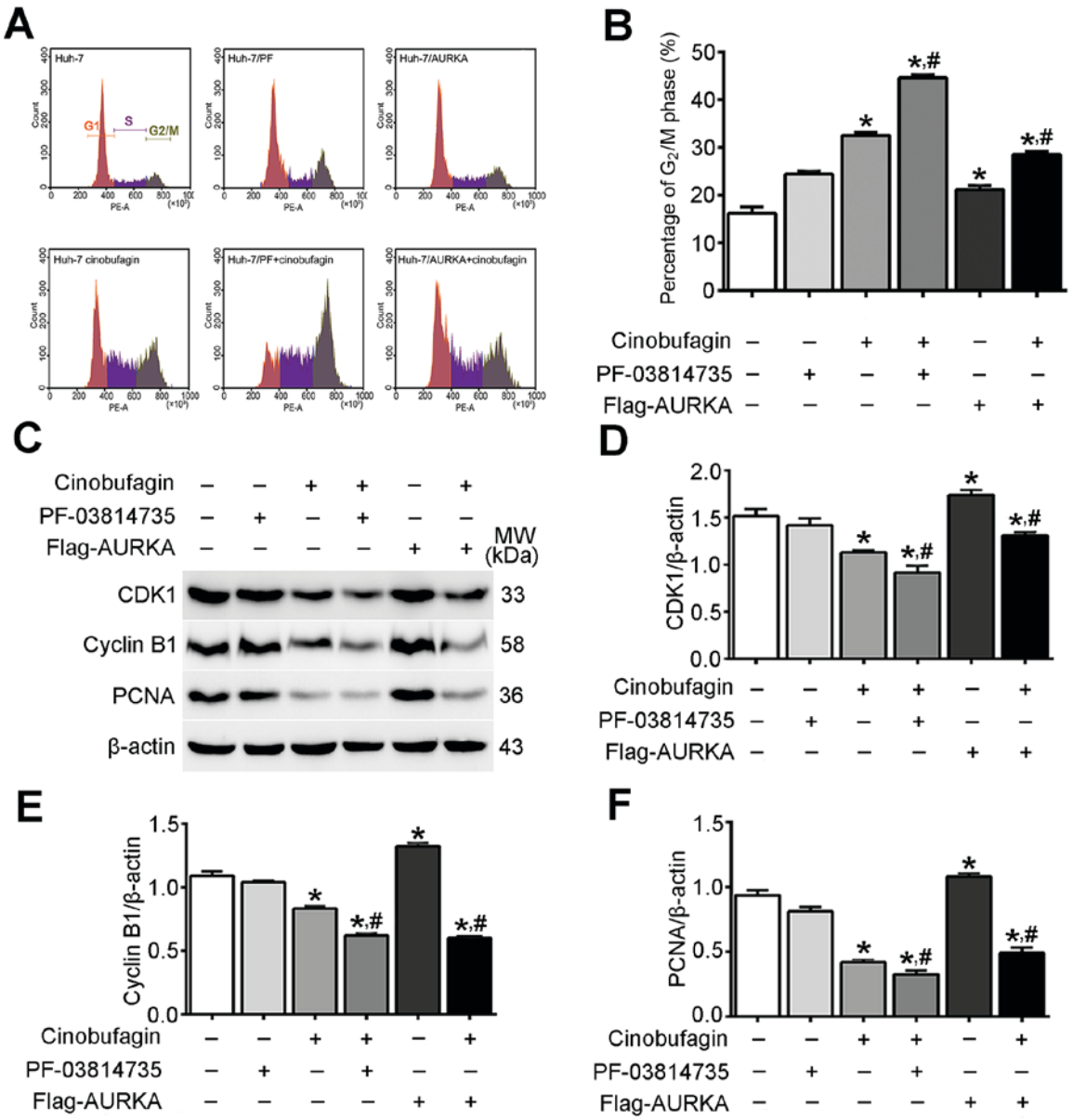

Figure 3. Cinobufagin induces cell cycle arrest at G_2/M phase. (A) Cell cycle distribution of Huh-7 cells following treatment with 5 μmol/l cinobufagin for 24 h, as determined using flow cytometry. (B) Cell cycle analysis of Huh-7 cells. (C) Protein expression levels of CDK1, cyclin B1 and PCNA following treatment with 5 μmol/l cinobufagin for 24 h. Densitometric analysis of (D) CDK1, (E) cyclin B1 and (F) PCNA. β-actin was used as a control. Data are presented as the means ± standard error of the mean of three independent experiments. *P<0.05 vs. control, #P<0.05 vs. cinobufagin. AURKA, aurora kinase A; CDK1, cyclin-dependent kinase 1; PCNA, proliferating cell nuclear antigen.

the Bcl-2/Bax ratio was significantly decreased following cinobufagin treatment compared with the control (P<0.05). Furthermore, the overexpression and inhibition of AURKA in cinobufagin-treated Huh-7 cells significantly increased and decreased the Bcl-2/Bax ratio compared with cinobufagin treatment alone, respectively (P<0.05). These results indicated that cinobufagin induced the apoptosis of Huh-7 cells in an AURKA-dependent manner.

Cinobufagin induces cell cycle arrest in Huh-7 cells by inhibition of AURKA signaling. As presented in Fig. 3A, cinobufagin induced the arrest of Huh-7 cells in G_2/M phase. The proportion of cells in the G_2/M phase was 16.17±0.77, 24.39±0.35 and 21.14±0.48 in the control, PF-03814735-treated and Flag-AURKA-transfected groups, respectively; treatment with cinobufagin increased the proportions in the respective groups to 32.52±0.34, 44.58±0.41 and 28.53±0.31%. The proportion of cells in G_2/M phase in the cinobufagin group was significantly increased compared with in the control group (P<0.05; Fig. 3B). Additionally, overexpressing or inhibiting AURKA in cinobufagin-treated Huh-7 cells significantly decreased or increased the proportion of G_2/M phase cells, respectively, compared with cinobufagin treatment alone (P<0.05). Western blot analysis revealed that cinobufagin decreased the expression levels of cyclin-dependent kinase 1 (CDK1), cyclin B1 and proliferating cell nuclear antigen (PCNA) in Huh-7 cells compared with the control (P<0.05; Fig. 3C-F). Additionally, overexpression or inhibition of AURKA in cinobufagin-treated Huh-7 cells significantly promoted or weakened the changes in the expression of these changed proteins between Huh-7 cells treated with cinobufagin and the control group, respectively (P<0.05).

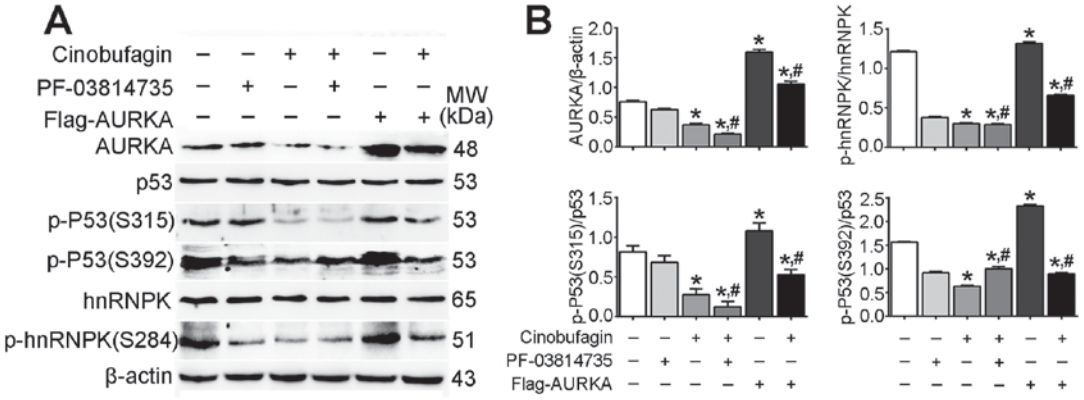

Figure 4. Anticancer effects of cinobufagin on Huh-7 cells are not dependent on the activation of p53 signaling. (A) Protein expression levels of AURKA, p53, p-p53 (S315), p-p53 (S392), hnRNPK and p-hnRNPK (S284) in cells following treatment with 5 μmol/l cinobufagin, as determined using western blotting. (B) Densitometric analysis of AURKA, p-p53 and p-hnRNPK. Data are presented as the means ± standard error of the mean of three independent experiments. *P<0.05 vs. control, #P<0.05 vs. cinobufagin. AURKA, aurora kinase A; hnRNPK, heterogeneous nuclear ribonucleoprotein K; p, phosphorylated.

The results indicated that cinobufagin induced cell cycle G_2/M phase arrest in Huh-7 cells via downregulation of CDK1, cyclin B1 and PCNA in an AURKA-dependent manner.

Anticancer effects of cinobufagin on Huh-7 cells are not dependent on the activation of p53 signaling. The present study revealed that the expression levels of total p53 and hnRNPK were not affected following cinobufagin treatment, or overexpression or inhibition of AURKA (Fig. 4A). Conversely, the expression levels of AURKA, p-p53 (S315), p-p53 (S392) and p-hnRNPK were significantly downregulated in cinobufagin-treated Huh-7 cells compared with the control (P<0.05; Fig. 4B). The expression of AURKA was significantly upregulated following transfection with the Flag-AURKA vector. Additionally, it was demonstrated that p-p53 (S315)/p53, p-p53 (S392)/p53 and p-hnRNPK (S284)/hnRNPK ratios were significantly decreased following cinobufagin treatment compared with the control. Overexpression and inhibition of AURKA in cinobufagin-treated cells significantly increased and decreased the p-p53 (S315)/p53 ratio compared with cinobufagin treatment alone, respectively; however, the p-p53 (S392)/p53 ratio was significantly increased in cinobufagin-treated cells following transfection with Flag-AURKA or treatment with PF-03814735 compared with cinobufagin treatment alone, whereas the p-hnRNPK (S284)/hnRNPK ratio was not significantly different between the cinobufagin and cinobufagin + PF-03814735 groups. The results suggested that cinobufagin downregulated the expression of AURKA, and inhibited the phosphorylation of p53 (S315 and S392) and hnRNPK (S284). Furthermore, overexpression of AURKA upregulated phosphorylation of p53 (S315), p53 (S392) and hnRNPK (S284) compared with cinobufagin treatment; however, PF-03814735 + cinobufagin treatment further decreased the phosphorylation of p53 (S315) only. Notably, the expression of total p53 was not altered, and the levels of p-p53 (S315 and S392) were significantly decreased in the cinobufagin group. The ratios of p-P53(S315)/p53 and p-P53(S392)/p53 in Huh-7 treated with cinobufagin were significantly decreased compared with the control group (P<0.05). Compared with Huh-7 treated with cinobufagin, the ratio of p-P53(S315)/p53 was significantly decreased, and the ratio of p-P53(S392)/p53 was significantly increased in Huh-7 cells treated with PF-03814735 + cinobufagin treatments (P<0.05). However, compared with Huh-7 cells treated with cinobufagin, the ratios of p-P53(S315)/p53 and p-P53(S392)/p53 in Flag-AURKA-transfected Huh-7 cells treated with cinobufagin were significantly increased (P<0.05), compared with the classic anticancer signaling of p53 (27,28).

Anticancer properties of cinobufagin in Huh-7 cells are associated with the activation of p73 signaling. Dabiri *et al* (29) demonstrated that p73 served as a substitute for p53 in bortezomib-induced apoptosis in p53-deficient or mutated cells, implicating that p73 could be a potential therapeutic target for treatment of colorectal cancer, in particular those lacking functional p53. The somatic mutation frequency of p53 is 11.2% in Huh-7 cells (30). It was hypothesized that the p53 mutation may result in a loss of function, leading to p53 losing its tumor-suppressive properties and acting as an oncogene. p73 is a proapoptotic protein that serves an important role during tumorigenesis, mimicking the tumor suppressor activities of p53 due to its structural similarity (31). The p-p73 (Y99)/p73 ratio was significantly increased in Huh-7 cells following cinobufagin treatment compared with the control, whereas that of p-MDM2 (S166)/MDM2 was significantly decreased (Fig. 5). Additionally, cinobufagin upregulated the expression of p21, Puma and Noxa compared with the control (P<0.05). Furthermore, the overexpression or inhibition of AURKA reduced or promoted the effects of cinobufagin, respectively (P<0.05).

Immunocytochemistry demonstrated that cinobufagin treatment markedly upregulated p73 expression compared with the control, whereas overexpression or inhibition of AURKA eliminated or promoted these cinobufagin-induced effects (Fig. 5G). These results indicated that the anticancer effects of cinobufagin in p53-mutant HCC cells were associated with the activation of p73, but not p53 signaling.

Discussion

At present, only 10-20% of patients with HCC can be treated surgically, whereas the majority of patients are treated exclusively with chemotherapy (2); However, the treatment of HCC

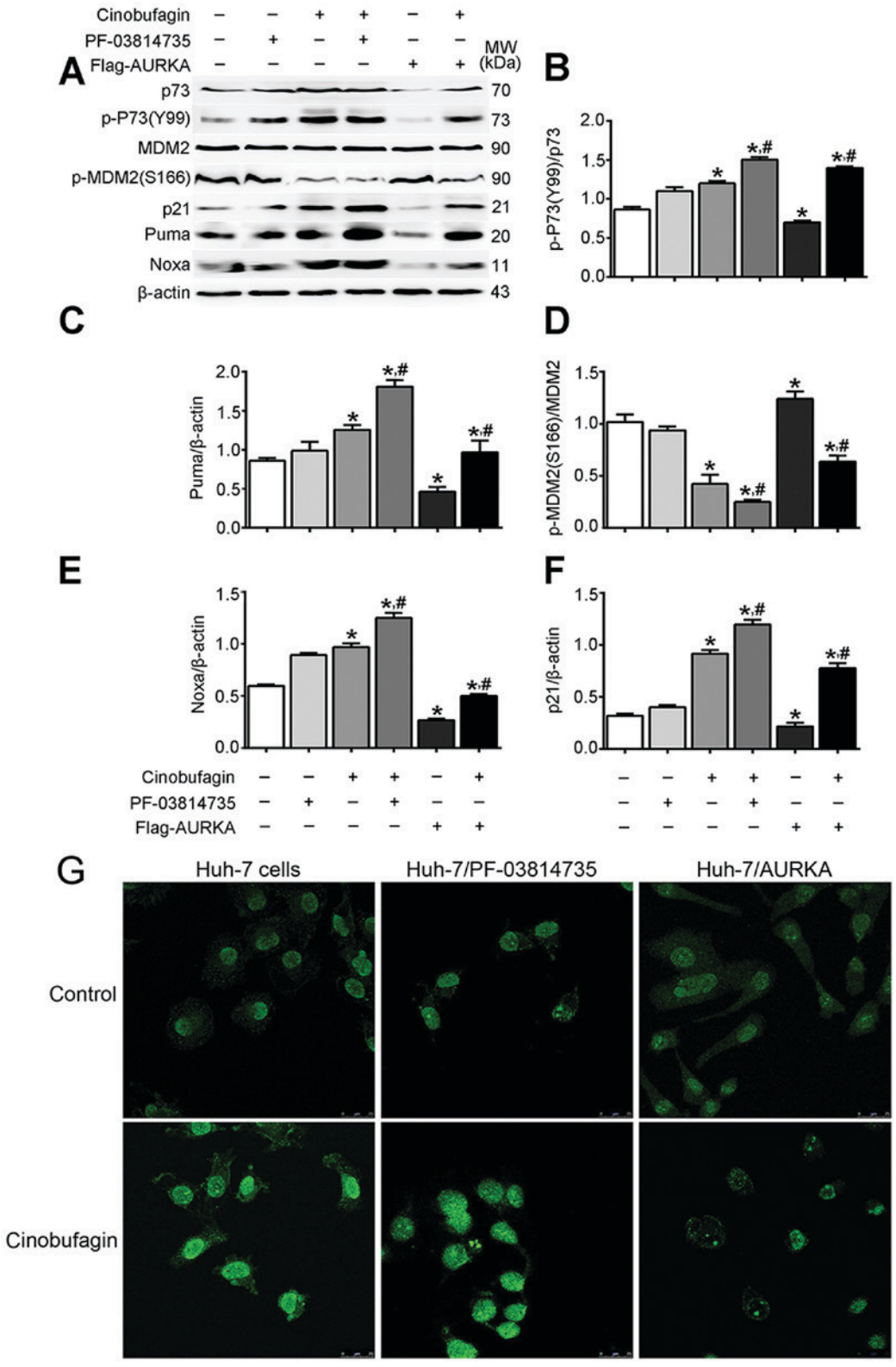

Figure 5. Cinobufagin may induce anticancer effects on Huh-7 cells via activation of p73 signaling. (A) Protein expression levels of p73, p-p73 (Y99), MDM2, p-MDM2 (S166), p21, Puma and Noxa in cells in cells following treatment with 5 μmol/l cinobufagin for 24 h, as determined by western blotting. Densitometric analysis of (B) p-p73, (C) Puma, (D) p-MDM2, (E) Noxa and (F) p21. (G) Expression of p73 in Huh-7 cells, as determined by immunocytochemistry. Representative images are shown at x200 magnification. Data are presented as the means ± standard error of the mean of three independent experiments. *P<0.05 vs. control, $^{\#}$P<0.05 vs. cinobufagin. AURKA, aurora kinase A; MDM2, mouse double minute 2 homolog; Noxa, phorbol-12-myristate-13-acetate-induced protein 1; p, phosphorylated; Puma, p53 upregulated modulator of apoptosis.

with anticancer agents, including sorafenib, capecitabine and oxaliplatin, is limited by multidrug resistance and individual heterogeneity (32). Notably, numerous studies have reported that CGs, as NKA inhibitors, exert anticancer properties against various types of cancer that are not susceptible to chemotherapy (33,34). CGs are synthetic or naturally

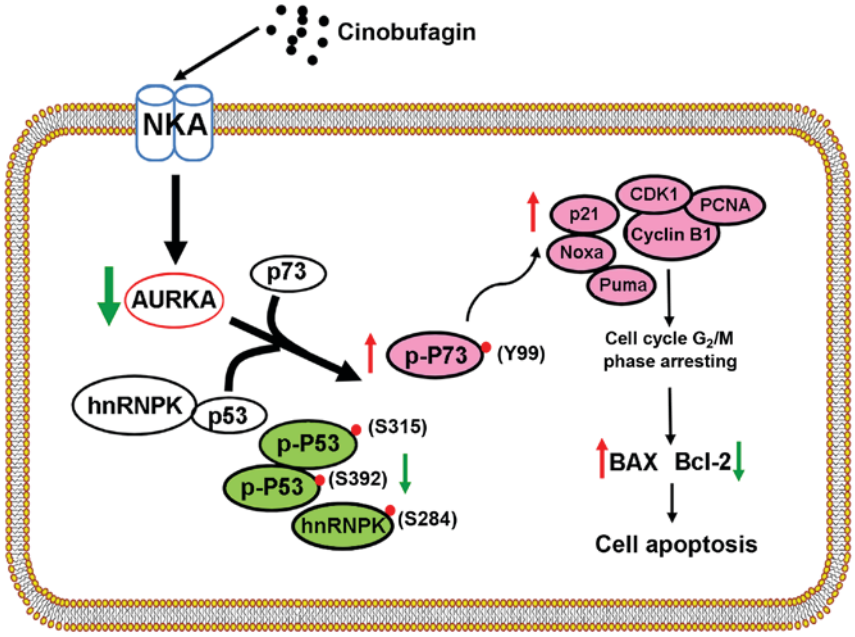

Figure 6. Schematic diagram of cinobufagin-induced effects on hepatocellular carcinoma Huh-7 cells with mutant p53. Cinobufagin inhibits the viability, arrests the cell cycle and induces the apoptosis of Huh-7 cells by inhibiting AURKA and p53 signaling, and activating p73 signaling. AURKA, aurora kinase A; Bax, Bcl-2-associated X protein; Bcl-2, B-cell lymphoma 2; CDK1, cyclin-dependent kinase 1; hnRNPK, heterogeneous nuclear ribonucleoprotein K; NKA, Na^+/K^+-ATPase; Noxa, phorbol-12-myristate-13-acetate-induced protein 1; p, phosphorylated; PCNA, proliferating cell nuclear antigen; Puma, p53 upregulated modulator of apoptosis.

occurring steroid hormones observed in plant or animal species, including ouabain, bufalin and cinobufagin (35). A number of studies reported that the survival rate of patients undergoing chemotherapy against HCC with mutant p53 is decreased compared with patients with wild-type p53 (26,36). Our previous study (14) revealed that CGs reduce the viability and induce the apoptosis of HCC cells with wild-type p53 by inhibiting AURKA signaling. In the present study, the anticancer effects of CGs were investigated in HCC Huh-7 cells with mutant p53.

Previous studies have reported that the overexpression or abnormal amplification of AURKA may serve an important role in the pathogenesis of various types of cancer (20,37). AURKA is a serine/threonine kinase that phosphorylates numerous target proteins involved in the establishment of the mitotic spindle, centrosome duplication, centrosome separation and cytokinesis, including BRCA1 DNA repair associated, cell division cycle 25B, kinesin family member 2A, large tumor suppressor kinase 2, p53 and TPX2 microtubule nucleation factor (38). In the present study, it was demonstrated that cinobufagin reduced the viability, arrested the cell cycle and induced the apoptosis of Huh-7 HCC cells possessing mutant p53. Furthermore, the overexpression or inhibition of AURKA suppressed or promoted the anticancer effects of cinobufagin on Huh-7 cells. The cyclin B1/CDK1 complex is required for regulation of the G_2/M transition phase of the cell cycle (39). The present study demonstrated that cinobufagin induced cell cycle G_2/M arrest by downregulating the expression of cyclin B1, CDK1 and PCNA, and upregulating the expression of p21. Additionally, the expression levels of p53 in Huh-7 cells were markedly unaltered following cinobufagin treatment, whereas the expression of p-p53 (S315) was significantly decreased. Therefore, it was suggested that the anticancer effects of cinobufagin in Huh-7 cells with mutant p53 did not depend on activation of the p53 signaling pathway.

Our previous study reported that the expression levels of p53 are significantly increased in HepG2 cells with wild-type p53 following CG treatment (14); however, the present study revealed that the expression of p53 was not significantly altered in CG-treated Huh-7 cells, and that the phosphorylation levels of p53 (S315 and S392) were decreased. Li *et al* (26) observed that the wild type p53 could inhibit cell proliferation and colony formation, but mutant p53 served a pro-oncogene function in several kinds of cancer cells. A separate study demonstrated that mutant p53 (R175H) exhibits pro-oncogenic properties, increasing the sensitivity of malignant ovarian cancer cells to growth factors and promoting their growth (40). Numerous studies revealed that p53, but not p73, is frequently mutated during tumorigenesis (41,42).

As a member of the p53 family, p73, a proapoptotic protein, serves an important role during tumorigenesis, mimicking the biological activities of p53 as a result of their structural similarity (43). Previous studies have reported that the knockdown of AURKA can induce increased p73 expression and increase the expression levels of its downstream molecules, including p21/WAF1, PUMA and Noxa (44,45). Meanwhile, Y99 phosphorylation of p-73 could bind to the PUMA promoter to induce PUMA expression, leading to apoptosis induction in cancer cells (46). In the present study, it was revealed that cinobufagin downregulated AURKA expression, and increased the expression and phosphorylation (Y99) levels of p73. MDM2 is an E3 ubiquitin ligase localized to the nucleus that inhibits p73-mediated cell cycle arrest and apoptosis by binding its transcriptional activation

domain (47). The present study revealed that cinobufagin inhibited the phosphorylation of MDM2. The upregulation of p-p73 increased the expression levels of downstream molecules, including Puma, Noxa and p21. Puma binds antiapoptotic Bcl-2 family members to induce mitochondrial dysfunction and caspase activation (48). Noxa promotes alterations in the mitochondrial membrane and the release of apoptogenic proteins from the mitochondria (49). p21 binds and inhibits the activity of CDK2 or CDK4, thereby regulating cell cycle progression (50). Additionally, it was demonstrated that the overexpression or inhibition of AURKA significantly opposed or promoted the anticancer effects of cinobufagin in Huh-7 cells, respectively.

Based on these findings, a schematic diagram was produced to present the hypothesized mechanisms underlying the anticancer effects of cinobufagin in Huh-7 cells, including inhibition of AURKA and p53 signaling, and activation of p73 signaling, which is associated with the activity of AURKA (Fig. 6). These results indicated that cinobufagin has potential as a novel anticancer agent for the treatment of patients with HCC possessing mutant p53. Future studies aim to establish animal models to further investigate the anticancer mechanisms of CGs.

Acknowledgements

Not applicable.

Funding

The present study was supported by the National Natural Science Foundation of China (grant nos. 81273552, 81673651 and 81273745) and the Natural Science Foundation of Tianjin City (grant nos. 18JCZDJC36500 and 11JCYBJC10900).

Availability of data and materials

The datasets used and/or analyzed during the current study are available from the corresponding author on reasonable request.

Authors' contributions

FW and ED were responsible for study design. LZ, LF and ZX performed the experiments and completed the manuscript draft. RFa, RX, RFu, SZ, CW, YaZ, JW, JB, ZW, XH and YuZ conducted data interpretation and analysis. All authors have read and approved the final manuscript.

Ethics approval and consent to participate

Not applicable.

Patient consent for publication

Not applicable.

Competing interests

The authors declare that they have no competing interests.

References

1. Clark T, Maximin S, Meier J, Pokharel S and Bhargava P: Hepatocellular carcinoma: Review of epidemiology, screening, imaging diagnosis, response assessment, and treatment. Curr Probl Diagn Radiol 44: 479-486, 2015.
2. Roxburgh P and Evans TR: Systemic therapy of hepatocellular carcinoma: Are we making progress? Adv Ther 25: 1089-1104, 2008.
3. Baek SH, Kim C, Lee JH, Nam D, Lee J, Lee SG, Chung WS, Jang HJ, Kim SH and Ahn KS: Cinobufagin exerts anti-proliferative and pro-apoptotic effects through the modulation ros-mediated mapks signaling pathway. Immunopharmacol Immunotoxicoz 37: 265-273, 2015.
4. Yu CH, Kan SF, Pu HF, Jea Chien E and Wang PS: Apoptotic signaling in bufalin- and cinobufagin-treated androgen-dependent and -independent human prostate cancer cells. Cancer Sci 99: 2467-2476, 2008.
5. Pereira DG, Salgado MAR, Rocha SC, Santos HL, Villar JAFP, Contreras RG, Fontes CFL, Barbosa LA and Cortes VF: Involvement of Src signaling in the synergistic effect between cisplatin and digoxin on cancer cell viability. J Cell Biochem 119: 3352-3362, 2018.
6. Gan PP, Zhou YY, Zhong MZ, Peng Y, Li L and Li JH: Endoplasmic reticulum stress promotes autophagy and apoptosis and reduces chemotherapy resistance in mutant p53 lung cancer cells. Cell Physiol Biochem 44: 133-151, 2017.
7. Bahrami A, Hesari A, Khazaei M, Hassanian SM, Ferns GA and Avan A: The therapeutic potential of targeting the braf mutation in patients with colorectal cancer. J Cell Physiol 233: 2162-2169, 2018.
8. Li BT, Ross DS, Aisner DL, Chaft JE, Hsu M, Kako SL, Kris MG, Varella-Garcia M and Arcila ME: Her2 amplification and her2 mutation are distinct molecular targets in lung cancers. J Thorac Oncol 11: 414-419, 2016.
9. Zhu VW, Cui JJ, Fernandez-Rocha M, Schrock AB, Ali SM and Ou SI: Identification of a novel t1151k alk mutation in a patient with alk-rearranged nsclc with prior exposure to crizotinib and ceritinib. Lung Cancer 110: 32-34, 2017.
10. Kang N, Wang Y, Guo S, Ou Y, Wang G, Chen J, Li D and Zhan Q: Mutant TP53 G245C and R273H promote cellular malignancy in esophageal squamous cell carcinoma. BMC Cell Biol 19: 16, 2018.
11. Tuna M, Amos CI and Mills GB: Genome-wide analysis of head and neck squamous cell carcinomas reveals HPV, TP53, smoking and alcohol-related allele-based acquired uniparental disomy genomic alterations. Neoplasia 21: 197-205, 2019.
12. Amelio I, Mancini M, Petrova V, Cairns RA, Vikhreva P, Nicolai S, Marini A, Antonov AA, Le Quesne J, Baena Acevedo JD, *et al*: p53 mutants cooperate with HIF-1 in transcriptional regulation of extracellular matrix components to promote tumor progression. Proc Natl Acad Sci USA 115: E10869-E10878, 2018.
13. Na K, Sung JY and Kim HS: Tp53 mutation status of tubo-ovarian and peritoneal high-grade serous carcinoma with a wild-type p53 immunostaining pattern. Anticancer Res 37: 6697-6703, 2017.
14. Xu Z, Wang F, Fan F, Gu Y, Shan N, Meng X, Cheng S, Liu Y, Wang C, Song Y and Xu R: Quantitative proteomics reveals that the inhibition of na(+)/k(+)-atpase activity affects s-phase progression leading to a chromosome segregation disorder by attenuating the aurora a function in hepatocellular carcinoma cells. J Proteome Res 14: 4594-4602, 2015.
15. Goos JA, Coupe VM, Diosdado B, Delis-Van Diemen PM, Karga C, Beliën JA, Carvalho B, van den Tol MP, Verheul HM, Geldof AA, *et al*: Aurora kinase a (AURKA) expression in colorectal cancer liver metastasis is associated with poor prognosis. Br J Cancer 109: 2445-2452, 2013.
16. Woo JK, Kang JH, Shin D, Park SH, Kang K, Nho CW, Seong JK, Lee SJ and Oh SH: Daurinol enhances the efficacy of radiotherapy in lung cancer via suppression of aurora kinase A/B expression. Mol Cancer Ther 14: 1693-1704, 2015.
17. Treekitkarnmongkol W, Katayama H, Kai K, Sasai K, Jones JC, Wang J, Shen L, Sahin AA, Gagea M, Ueno NT, *et al*: Aurora kinase-a overexpression in mouse mammary epithelium induces mammary adenocarcinomas harboring genetic alterations shared with human breast cancer. Carcinogenesis 37: 1180-1189, 2016.
18. Zhang J, Li B, Yang Q, Zhang P and Wang H: Prognostic value of aurora kinase a (AURKA) expression among solid tumor patients. A systematic review and meta-analysis. Jpn J Clin Oncol 45: 629-636, 2015.

19. Lo Iacono M, Monica V, Saviozzi S, Ceppi P, Bracco E, Papotti M and Scagliotti GV: Aurora kinase a expression is associated with lung cancer histological-subtypes and with tumor de-differentiation. J Transl Med 9: 100, 2011.
20. Chen C, Song G, Xiang J, Zhang H, Zhao S and Zhan Y: AURKA promotes cancer metastasis by regulating epithelial-mesenchymal transition and cancer stem cell properties in hepatocellular carcinoma. Biochem Biophys Res Commun 486: 514-520, 2017.
21. Fischer M: Census and evaluation of p53 target genes. Oncogene 36: 3943-3956, 2017.
22. Yue X, Zhao Y, Xu Y, Zheng M, Feng Z and Hu W: Mutant p53 in cancer: Accumulation, gain-of-function, and therapy. J Mol Biol 429: 1595-1606, 2017.
23. Singh S, Vaughan CA, Frum RA, Grossman SR, Deb S and Palit Deb S: Mutant p53 establishes targetable tumor dependency by promoting unscheduled replication. J Clin Invest 127: 1839-1855, 2017.
24. Botchkarev VA and Flores ER: P53/p63/p73 in the epidermis in health and disease. Cold Spring Harb Perspect Med 4: pii: a015248, 2014.
25. Kasai F, Hirayama N, Ozawa M, Satoh M and Kohara A: HuH-7 reference genome profile: Complex karyotype composed of massive loss of heterozygosity. Hum Cell 31: 261-267, 2018.
26. Li Q, Liu X, Jin K, Lu M, Zhang C, Du X and Xing B: Nat10 is upregulated in hepatocellular carcinoma and enhances mutant p53 activity. BMC Cancer 17: 605, 2017.
27. Cavic M, Spasic J, Krivokuca A, Boljevic I, Kuburovic M, Radosavljevic D and Jankovic R: TP53 and DNA-repair gene polymorphisms genotyping as a low-cost lung adenocarcinoma screening tool. J Clin Pathol 72: 75-80, 2019.
28. Hsieh Li SM, Liu ST, Chang YL, Ho CL and Huang SM: Metformin causes cancer cell death through downregulation of p53-dependent differentiated embryo chondrocyte 1. J Biomed Sci 25: 81, 2018.
29. Dabiri Y, Kalman S, Gurth CM, Kim JY, Mayer V and Cheng X: The essential role of TAp73 in bortezomib-induced apoptosis in p53-deficient colorectal cancer cells. Sci Rep 7: 5423, 2017.
30. Kandoth C, McLellan MD, Vandin F, Ye K, Niu B, Lu C, Xie M, Zhang Q, McMichael JF, Wyczalkowski MA, *et al*: Mutational landscape and significance across 12 major cancer types. Nature 502: 333-339, 2013.
31. Zawacka-Pankau J, Kostecka A, Sznarkowska A, Hedström E and Kawiak A: P73 tumor suppressor protein: A close relative of p53 not only in structure but also in anti-cancer approach? Cell Cycle 9: 720-728, 2010.
32. Babula P, Masarik M, Adam V, Provaznik I and Kizek R: From na+/k+-atpase and cardiac glycosides to cytotoxicity and cancer treatment. Anticancer Agents Med Chem 13: 1069-1087, 2013.
33. Kaushik V, Yakisich JS, Azad N, Kulkarni Y, Venkatadri R, Wright C, Rojanasakul Y and Iyer AKV: Anti-tumor effects of cardiac glycosides on human lung cancer cells and lung tumorspheres. J Cell Physiol 232: 2497-2507, 2017.
34. Kaushik V, Azad N, Yakisich JS and Iyer AK: Antitumor effects of naturally occurring cardiac glycosides convallatoxin and peruvoside on human er+ and triple-negative breast cancers. Cell Death Discov 3: 17009, 2017.
35. Calderon-Montano JM, Burgos-Moron E, Orta ML, Maldonado-Navas D, Garcia-Dominguez I and Lopez-Lazaro M: Evaluating the cancer therapeutic potential of cardiac glycosides. Biomed Res Int 2014: 794930, 2014.
36. Zhang ZY, Hong D, Nam SH, Kim JM, Paik YH, Joh JW, Kwon CH, Park JB, Choi GS, Jang KY, *et al*: Sirt1 regulates oncogenesis via a mutant p53-dependent pathway in hepatocellular carcinoma. J Hepatol 62: 121-130, 2015.
37. Li T, Chen Y, Zhang J and Liu S: LncRNA TUG1 promotes cells proliferation and inhibits cells apoptosis through regulating AURKA in epithelial ovarian cancer cells. Medicine (Baltimore) 97: E12131, 2018.
38. Zheng F, Yue C, Li G, He B, Cheng W, Wang X, Yan M, Long Z, Qiu W, Yuan Z, *et al*: Nuclear aurka acquires kinase-independent transactivating function to enhance breast cancer stem cell phenotype. Nat Commun 7: 10180, 2016.
39. Lee MH, Cho Y, Kim DH, Woo HJ, Yang JY, Kwon HJ, Yeon MJ, Park M, Kim SH, Moon C, *et al*: Menadione induces G2/M arrest in gastric cancer cells by down-regulation of CDC25C and proteasome mediated degradation of CDK1 and cyclin B1. Am J Transl Res 8: 5246-5255, 2016.
40. Padmanabhan A, Candelaria N, Wong KK, Nikolai BC, Lonard DM, O'Malley BW and Richards JS: USP15-dependent lysosomal pathway controls p53-R175H turnover in ovarian cancer cells. Nat Commun 9: 1270, 2018.
41. Melino G, Bernassola F, Ranalli M, Yee K, Zong WX, Corazzari M, Knight RA, Green DR, Thompson C and Vousden KH: P73 induces apoptosis via puma transactivation and bax mitochondrial translocation. J Biol Chem 279: 8076-8083, 2004.
42. Yoon MK, Ha JH, Lee MS and Chi SW: Structure and apoptotic function of p73. BMB Rep 48: 81-90, 2015.
43. Huang L, Li A, Liao G, Yang F, Yang J, Chen X and Jiang X: Curcumol triggers apoptosis of p53 mutant triple-negative human breast cancer MDA-MB 231 cells via activation of p73 and PUMA. Oncol Lett 14: 1080-1088, 2017.
44. Katayama H, Wang J, Treekitkarnmongkol W, Kawai H, Sasai K, Zhang H, Wang H, Adams HP, Jiang S, Chakraborty SN, *et al*: Aurora kinase-A inactivates DNA damage-induced apoptosis and spindle assembly checkpoint response functions of p73. Cancer Cell 21: 196-211, 2012.
45. Dar AA, Belkhiri A, Ecsedy J, Zaika A and El-Rifai W: Aurora kinase a inhibition leads to p73-dependent apoptosis in p53-deficient cancer cells. Cancer Res 68: 8998-9004, 2008.
46. Riley MF, You MJ, Multani AS and Lozano G: Mdm2 overexpression and p73 loss exacerbate genomic instability and dampen apoptosis, resulting in B-cell lymphoma. Oncogene 35: 358-365, 2016.
47. Knickelbein K, Tong J, Chen D, Wang YJ, Misale S, Bardelli A, Yu J and Zhang L: Restoring PUMA induction overcomes KRAS-mediated resistance to anti-EGFR antibodies in colorectal cancer. Oncogene 37: 4599-4610, 2018.
48. Bean GR, Ganesan YT, Dong Y, Takeda S, Liu H, Chan PM, Huang Y, Chodosh LA, Zambetti GP, Hsieh JJ and Cheng EH: PUMA and BIM are required for oncogene inactivation-induced apoptosis. Sci Signal 6: ra20, 2013.
49. Guikema JE, Amiot M and Eldering E: Exploiting the pro-apoptotic function of NOXA as a therapeutic modality in cancer. Expert Opin Ther Targets 21: 767-779, 2017.
50. Cazzalini O, Scovassi AI, Savio M, Stivala LA and Prosperi E: Multiple roles of the cell cycle inhibitor p21(CDKN1A) in the DNA damage response. Mutat Res 704: 12-20, 2010.